Genetic analysis of zebrafish homologs of human FOXQ1, *foxq1a* and *foxq1b*, in innate immune cell development and bacterial host response

Alison M. Earley, Cameron T. Dixon, Celia E. Shiau*

Department of Biology, University of North Carolina at Chapel Hill, Chapel Hill, NC, United States of America

* shiauce@unc.edu

Abstract

FOXQ1 is a member of the forkhead-box transcription factor family that has important functions in development, cancer, aging, and many cellular processes. The role of FOXQ1 in cancer biology has raised intense interest, yet much remains poorly understood. We investigated the possible function of the two zebrafish orthologs (*foxq1a* and *foxq1b*) of human FOXQ1 in innate immune cell development and function. We employed CRISPR-Cas9 targeted mutagenesis to create null mutations of *foxq1a* and *foxq1b* in zebrafish. Using a combination of molecular, cellular, and embryological approaches, we characterized single and double *foxq1a* [bcz11] and *foxq1b* [bcz18] mutants. This study provides the first genetic mutant analyses of zebrafish *foxq1a* and *foxq1b*. Interestingly, we found that *foxq1a*, but not *foxq1b*, was transcriptionally regulated during a bacterial response, while the expression of *foxq1a* was detected in sorted macrophages and upregulated in *foxq1a*-deficient mutants. However, the transcriptional response to *E. coli* challenge of *foxq1a* and *foxq1b* mutants was not significantly different from that of their wildtype control siblings. Our data shows that *foxq1a* may have a role in modulating bacterial response, while both *foxq1a* and *foxq1b* are not required for the development of macrophages, neutrophils, and microglia. Considering the implicated role of FOXQ1 in a vast number of cancers and biological processes, the *foxq1a* and *foxq1b* null mutants from this study provide useful genetic models to further investigate FOXQ1 functions.

Introduction

FOXQ1 is a member of the forkhead-box (FOX) transcription factor gene family, which contains a winged helix DNA binding domain and has important functions in development, cancer, aging, cell cycle regulation, cell migration, and other diverse cellular processes [1–5]. Previous studies in mammals show that the functions of FOXQ1 include promoting epithelial differentiation [6–11], inhibiting smooth muscle differentiation [12], mediating hair development [13,14], controlling gastric acid production and secretion in stomach mucous cells [15,16], regulating

glucose metabolism [17], as well as possible immunological functions [18,19]. Additionally, upregulation of FOXQ1 is found in a large host of cancer types, possibly to regulate cell proliferation and invasion, including breast [7,20,21], colorectal [22–25], pancreatic [26,27], gastric [28–31], bladder [32], liver [33–36], lung [37,38], ovarian [39,40], and glioma [41]. With these findings, FOXQ1 has generated much interest into its functions and mechanisms.

In light of the interactions of innate immune cells, particularly macrophages, in tumor development, progression, and metastasis [42–48], and possible roles of FOXQ1 in regulating these processes [49,50], we generated gene knockouts of the two zebrafish orthologs (*foxq1a* and *foxq1b*) of human FOXQ1 using CRIPSR-Cas9 targeted mutagenesis. Using single and double *foxq1a* and *foxq1b* mutants, we investigated whether FOXQ1 is critical for the development and function of macrophages and other innate immune cells. Establishing a function for FOXQ1 in innate immune regulation can provide new understanding of its role in various cancers.

This study provides the first genetic mutant analyses of zebrafish *foxq1a* and *foxq1b*. We found RNA expression of both copies of *foxq1* in the developing craniofacial structures as previously reported [51,52], in addition to *foxq1a* expression in sorted macrophages as well as in the yolk region. Neither single nor double *foxq1a* and *foxq1b* mutants had overt gross morphological defects or notable deficiency in the development of macrophages, neutrophils, and microglia. Furthermore, *foxq1a* and *foxq1b* mutants exhibited a typical transcriptional response to bacterial challenge, but *foxq1a* is interestingly downregulated during this response in wildtype. Considering the implicated role of FOXQ1 in a vast number of cancers and biological processes, the *foxq1a* and *foxq1b* mutants generated in this study provide new genetic models to further dissect the functions of FOXQ1.

Results

Generation of *foxq1a*^{bcz11} and *foxq1b*^{bcz18} null alleles using CRISPR-Cas9

We employed the highly effective CRISPR-Cas9 mediated targeted mutagenesis in zebrafish as previously described [53,54] to create loss-of-function mutations at the beginning of *foxq1a* and *foxq1b* genes. We isolated two mutant alleles of interest: *foxq1a*^{bcz11} and *foxq1b*^{bcz18} (Fig 1A). These are frameshift mutations that lead to a premature stop codon at the beginning of each respective gene: *bcz11* has a large 95 base pair (bp) deletion in *foxq1a* that is immediately followed by a premature stop codon, and *bcz18* has a 4 bp deletion and a 12 bp insertion in *foxq1b* that causes a premature stop codon within the start of the indel (Fig 1A). RT-PCR and sequencing analysis confirmed expression of the expected nonsense transcripts from the *bcz11* and *bcz18* mutations, and no alternative splicing was found (S1 Fig). The data indicate that *bcz11* and *bcz18* represent null alleles of their respective genes by producing nonsense mRNAs that would prevent Foxq1a and Foxq1b protein expression, respectively. For each gene target, three guide RNAs (gRNAs) were used in combination to increase the efficiency of the mutagenesis and the probability of generating a large indel mutation (Fig 1A). At 5 days post-fertilization (dpf) when zebrafish have well established organ systems and are free-swimming larvae, we examined the gross morphology of the homozygous mutants (Fig 1B). We found that both *foxq1a*^{bcz11} and *foxq1b*^{bcz18} homozygous mutants were indistinguishable from wildtype siblings (Fig 1B), displaying normal-sized inflated swim bladders, and grossly normal head and body structures that were no different from wildtype. However, we cannot exclude the possibility that craniofacial and specific organ phenotypes may be present in the mutants without further detailed analysis, in regions that normally express *foxq1a* and *foxq1b* [51,52]. The viability of *bcz11* and *bcz18* mutants, at least up to larval stages, appeared to be normal, as we consistently found ~25% of the progenies to be mutants from a heterozygous incross.
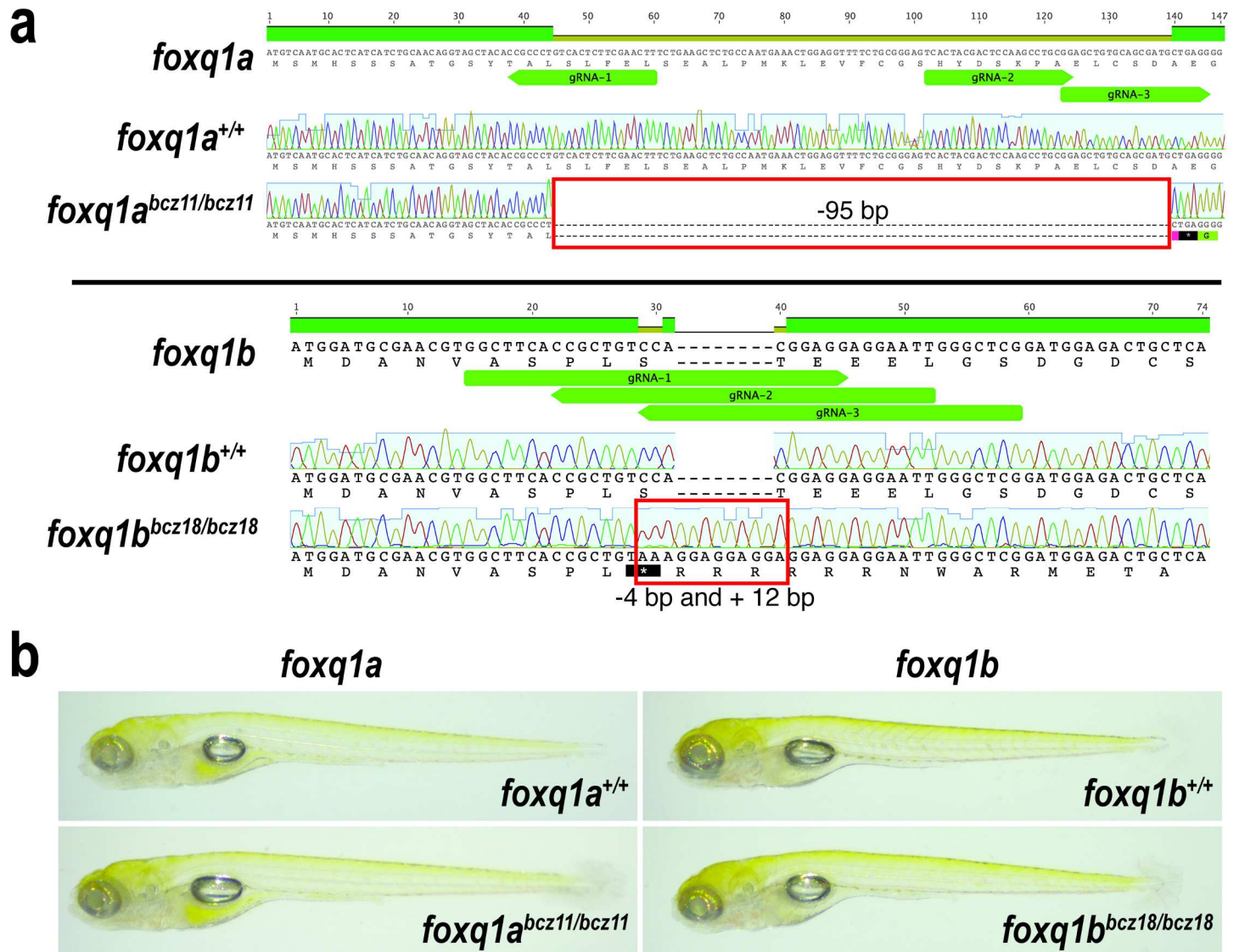
Fig 1. Sequence analysis of *foxq1a*^bcz11 and *foxq1b*^bcz18 mutations generated by CRISPR-Cas9 targeting. a Top, DNA and amino acid sequences of the 5' end of *foxq1a* coding region. DNA sequencing chromatograms show the expected foxq1a sequence in the wildtype sibling, and a large 95 base pair deletion (red box) in the homozygous *bcz11* mutant, which causes a premature stop (black box with an asterisk) at the beginning of the gene. Bottom, DNA and amino acid sequences of the 5' end of *foxq1b* coding region. DNA chromatograms show wildtype sequence in *foxq1b* wildtype sibling, while the homozygous *bcz18* mutant carries a 4 bp deletion and 12 bp insertion (red box) causing a nonsense mutation at the beginning of the gene. gRNA, target sites of the guide RNAs used. **b** Whole mount live imaging of 5 dpf larvae show normal gross morphological development of *foxq1a*^bcz11 and *foxq1b*^bcz18 mutants as compared to wildtype siblings (at least 10 animals were analyzed per genotype group).

Characterization of *foxq1a* and *foxq1b* gene expressions

The expression patterns of *foxq1a* and *foxq1b* in zebrafish remain largely unanalyzed. Only two studies to date have examined their expressions in specific tissues of interest; one showed *foxq1b* expression in the developing jaws at 2 dpf [51] and the other reported that *foxq1a* may be expressed in the cranial suture in juvenile zebrafish (6 weeks post-fertilization) [52]. To better define the possible functions of these genes in zebrafish, we expanded the characterization of their expressions to various stages of development from 1 to 8 dpf, and tested whether they were expressed in macrophages (Fig 2). Using fluorescence-activated cell sorting (FACS), we isolated macrophages (M) based on GFP expression from 2.5 dpf zebrafish embryos carrying
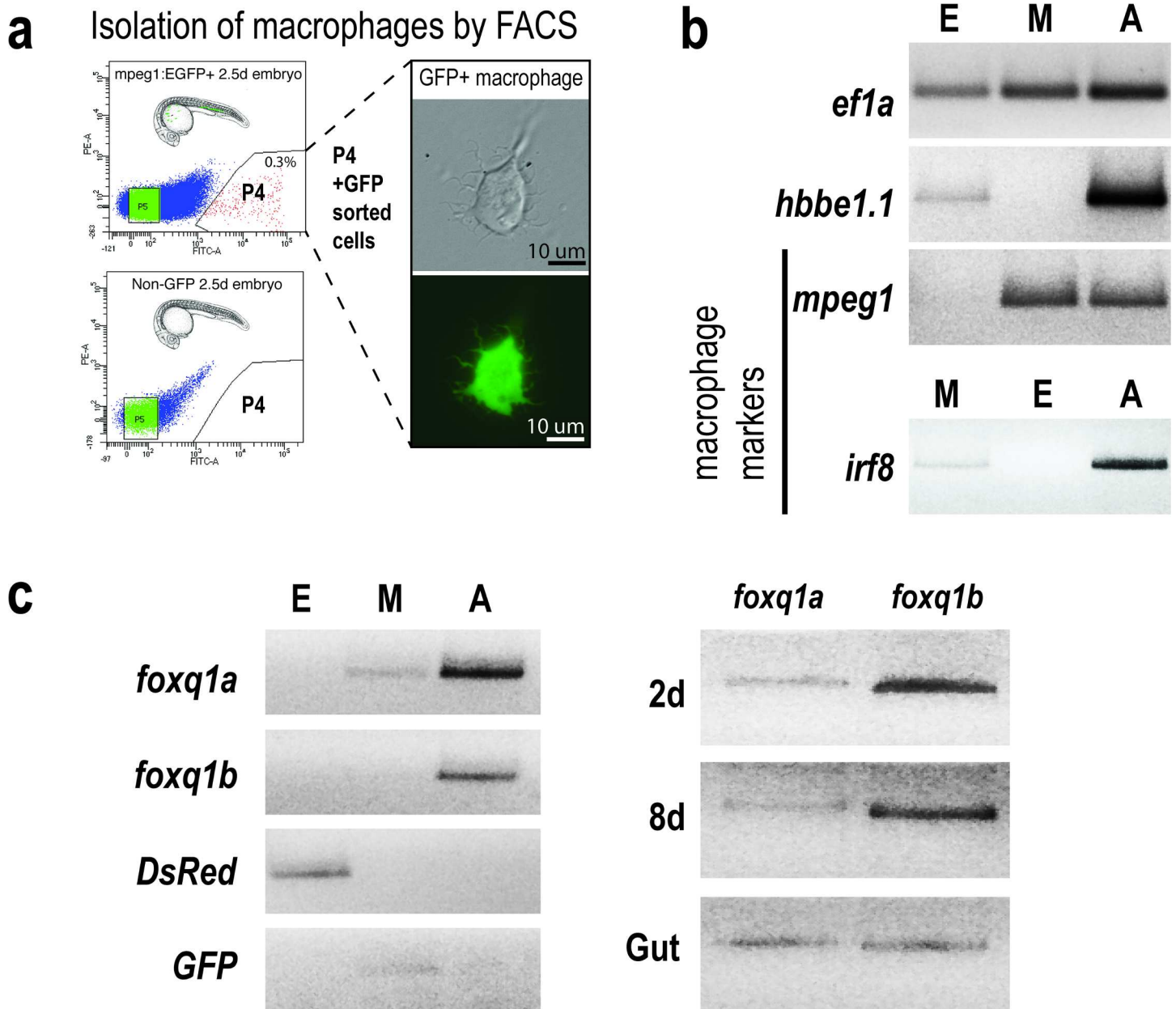
Fig 2. Gene expression analysis of *foxq1a* and *foxq1b*. a Isolation of macrophages based on GFP expression by FACS in *mpeg1:EGFP* transgenic zebrafish embryos at 2.5 dpf. Non-fluorescent embryos were used as a negative control for gating. Top left, P4 shows the cell fraction sorted as GFP+ macrophages, also shown in the right panels in brightfield and green channel. **b** RT-PCR analysis of gene markers validated the different cell populations sorted by FACS, as denoted by E, erythrocytes; M, macrophages; A, all remaining non-fluorescent cells. The following genes were used: translation elongation factor 1 (*ef1a*) as a reference marker, hemoglobin beta embryonic-1.1 (*hbbe1.1*) as an erythrocyte marker, and macrophage expressed gene 1 (*mpeg1*) and interferon regulatory factor 8 (*irf8*) as well-established macrophage markers in zebrafish. As expected, the 'A' cells expressed all genes, while erythrocytes 'E' cells expressed *hbbe1.1*, *ef1a*, and *DsRed* genes and macrophage 'M' cells expressed macrophage markers, *GFP*, and *ef1a*. **c** Using the sorted cell populations, we found expression of *foxq1a* in macrophages and neither gene in erythrocytes. Both genes are expressed at 2 to 8 dpf of development as well as in the adult gut tissue.

the macrophage-specific transgene *mpeg1:EGFP* (Fig 2A). To assess their expression in other cell types as additional references, we sorted erythrocytes (E) based on DsRed expression from erythrocyte-specific *gata1:DsRed* transgenic embryos as well as the remaining non-fluorescent cells (A) (Fig 2B and 2C). We verified the identity of the sorted cell populations by RT-PCR
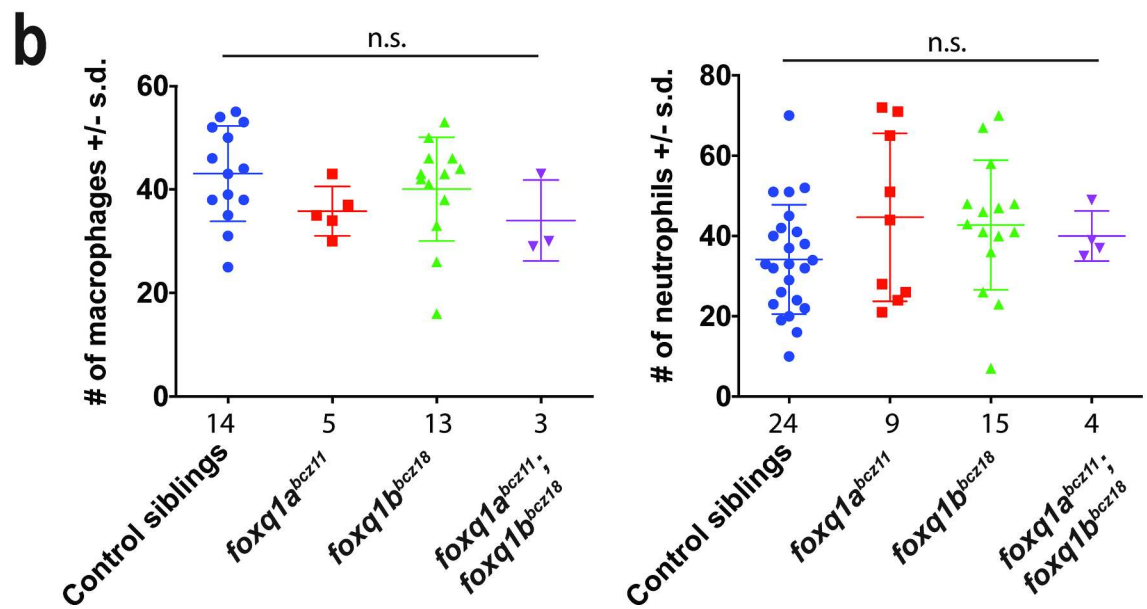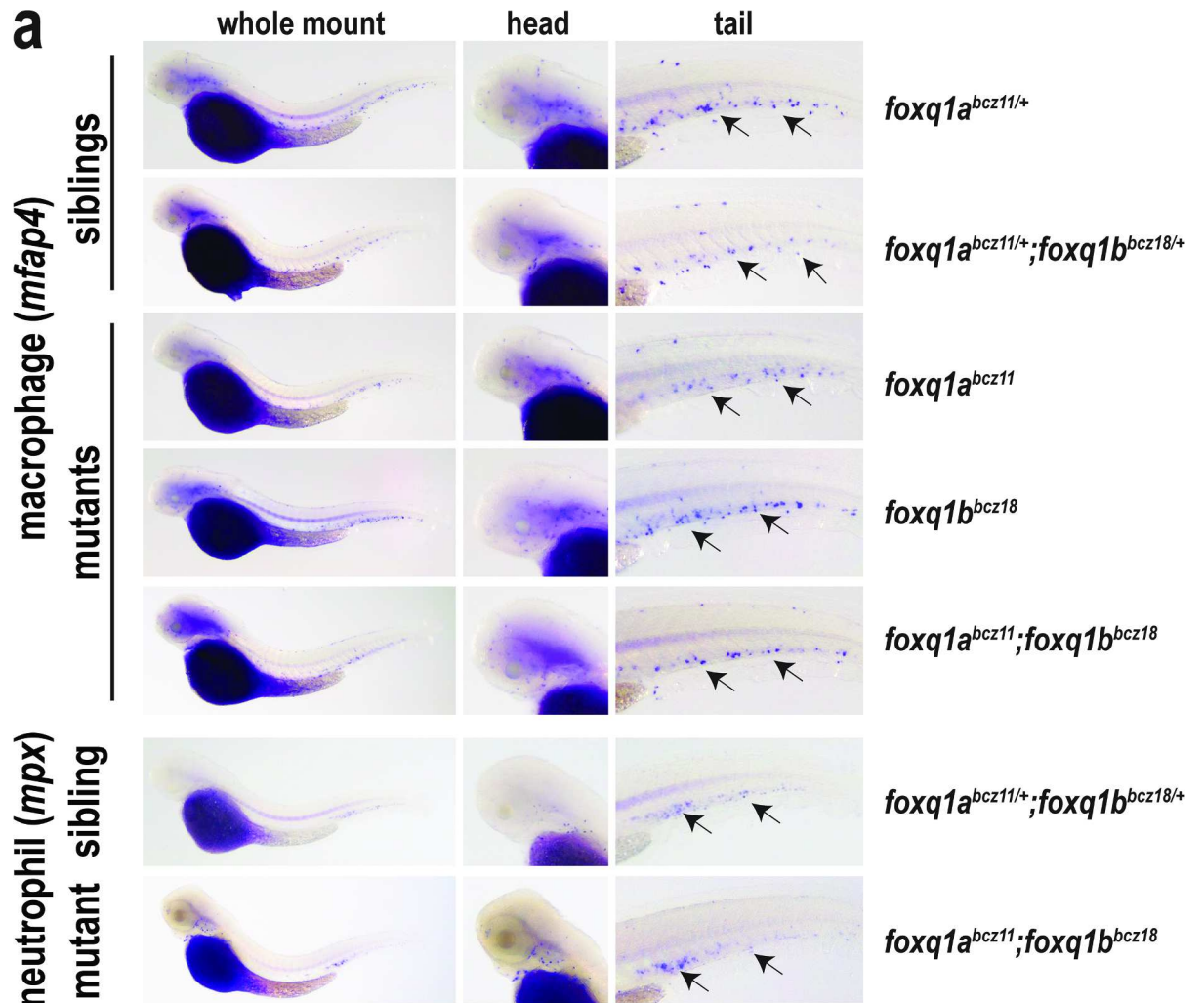
Fig 3. Single and double *foxq1a*^bcz11^ and *foxq1b*^bcz18^ mutants have normal macrophage and neutrophil development. a Whole mount *in situ* hybridization of 2.5 dpf single and double *foxq1a*^bcz11^ and *foxq1b*^bcz18^ mutants and their siblings using RNA probes for *mfap4* (macrophage marker) and *mpx* (neutrophil marker). Arrows, macrophages or neutrophils in the caudal hematopoietic tissue in the embryo tail. **b** Scatter plots showing number of macrophages and neutrophils in the tail region for each embryo quantified in the different genotype categories. n, number of embryos analyzed beneath each scatter plot. Plots report average ± standard deviation (s.d.). Multiple unpaired t-tests comparing between control siblings and each of the mutants groups were conducted with correction for multiple comparisons using the Sidak-Bonferroni method and without assuming equal variance to determine statistical significance. n.s., no statistical significance as defined by p > 0.05 was found in all the comparisons.

https://doi.org/10.1371/journal.pone.0194207.g003

analysis using known markers and fluorescent reporter genes for the E, M, and A cells (Fig 2B and 2C). The data shows that while both genes are expressed from 2 to 8 dpf (Fig 2C), only *foxq1a* is expressed by macrophages and neither gene is expressed by erythrocytes (Fig 2C). Using RNA *in situ* hybridization, we found expression of *foxq1a* in the cranial region at 1 dpf that persists in the jaw at 2.5 dpf when it is also found in the body tissue along the yolk, and on the yolk (S2 Fig). By contrast, *foxq1b* was primarily found to be expressed in the ventral jaw region at 2.5 dpf (S2 Fig). While *foxq1a* RNA expression was found in macrophages isolated from wildtype embryos (Fig 2C), its level may be too low to be detectable by whole mount RNA in situ hybridization as we were unable to visualize its expression in macrophages by *in situ* (S2 Fig). Because FOXQ1 is known to be highly expressed in the mammalian gastrointestinal tract [15,16,55,56], we examined whether *foxq1a* and *foxq1b* are expressed in the adult zebrafish gut, and indeed found them both to be expressed (Fig 2C).

Single and double *foxq1a*^bcz11^ and *foxq1b*^bcz18^ mutants show normal macrophage, neutrophil, and microglia development

In light of the finding that *foxq1a* is expressed in macrophages and the implicated mammalian FOXQ1 function in tumor biology that may involve innate immune cells [19], we asked whether the development of macrophages and neutrophils may be altered in the zebrafish *foxq1* mutants. By whole mount RNA in situ hybridization using a macrophage marker (*mfap4*) [57,58] and neutrophil marker (*mpx*) [59,60], we found no apparent difference in formation or distribution of these innate immune cells during development at 2.5 dpf in *foxq1a*^bcz11^ mutants and *foxq1b*^bcz18^ mutants (Fig 3A). In case of redundant or compensatory functions of *foxq1a* and *foxq1b*, we examined the double *foxq1a*^bcz11^;*foxq1b*^bcz18^ homozygous mutants, but also found no marked differences compared to wildtype siblings (Fig 3A). Quantification of macrophage and neutrophil numbers in the tail region further substantiates our finding that the mutants are not significantly different from siblings in innate immune cell development (Fig 3B). Since it is possible to have defects in macrophages at later time points, we evaluated the development of microglia, an important derivative of embryonic macrophages. We used a vital neutral red stain assay that has been shown to specifically label microglia in the larval zebrafish brain [61–63] as cells with dark red aggregates (Fig 4A). We found that all *foxq1a*^bcz11^, *foxq1b*^bcz18^ and *foxq1a*^bcz11^;*foxq1b*^bcz18^ mutants exhibited the typical pattern (Fig 4A) and numbers (Fig 4B) of microglia in the larval midbrain as those in wildtype and heterozygous control siblings and previously described for wildtype [61–65]. Taken together, the data indicates that *foxq1a* and *foxq1b* are not required for the proper development of macrophages, neutrophils, and microglia.

foxq1a and *foxq1b* null mutants exhibit typical transcriptional response to *Escherichia coli* brain challenge

While *foxq1a* and *foxq1b* are not essential for innate immune cell development, they may affect the function of these cells, such as their ability to mediate an immune response. We developed
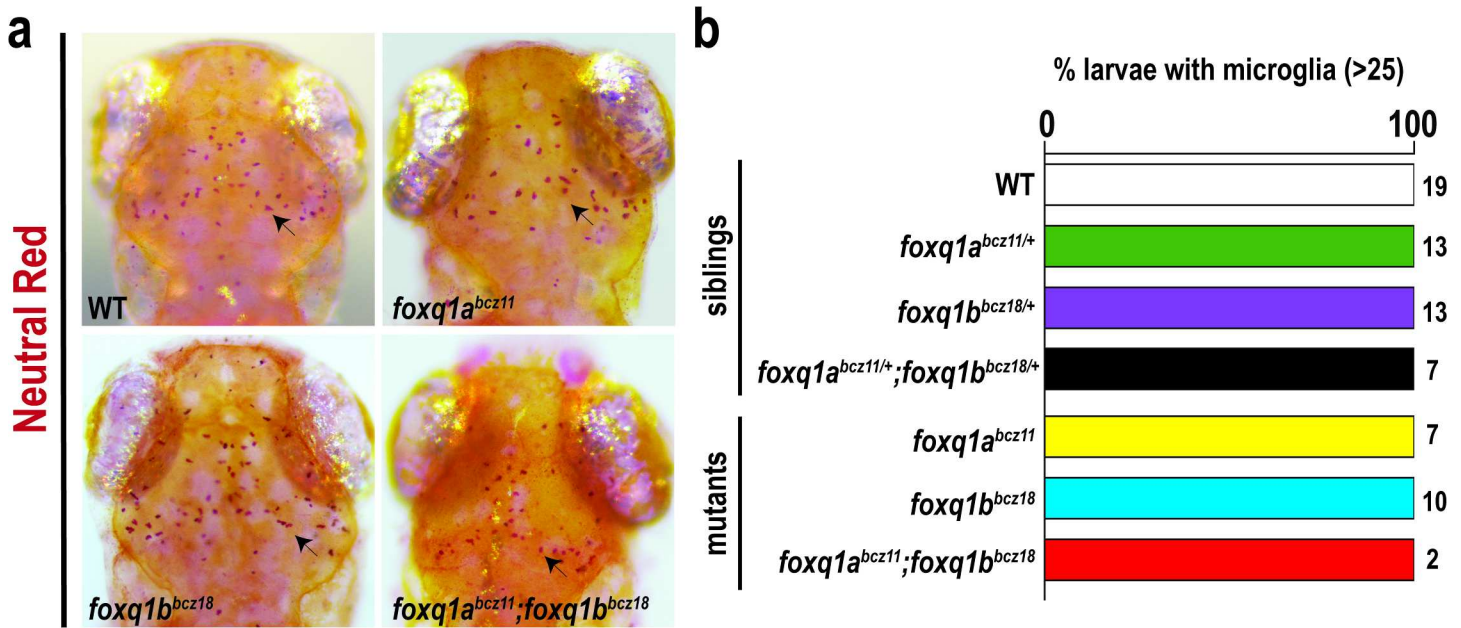
Fig 4. Neutral red analysis shows normal microglia development in single and double *foxq1a* and *foxq1b* mutants at 4 dpf. a Neutral red staining in 4 dpf wildtype (WT) sibling, *foxq1a^{bcz11}*, *foxq1b^{bcz18}*, and *foxq1a^{bcz11}*;*foxq1b^{bcz18}* mutants shows a stereotypical pattern of microglia in the midbrain (arrow). **b** Bar graph shows all larvae analyzed in all genotype groups had normal numbers of microglia (>25). Number of larvae analyzed (n) shown to the right of the corresponding bar.

a brain challenge assay (Fig 5A) to trigger innate immune activation by introducing live *E. coli* bacteria into the brain tectum of zebrafish larvae. We used this assay to address whether *foxq1a*, *foxq1b*, or both may regulate systemic response to *E. coli* challenge. We validated the effectiveness of our assay to trigger immune activation by showing that after brain challenge with bacteria or LPS at 6 hours post injection (hpi), we indeed found significant elevation of several innate immune activation genes systemically: interleukin 1 beta (*il1β*) [61,62,66], immune responsive gene (*irg1*) [67], neutrophil gene (*mpx*) [68], and tumor necrosis factor alpha (*tnfα*) [69] but not in water injected or uninjected controls (Fig 5B). We also tested whether *foxq1a* and *foxq1b* themselves could be transcriptionally regulated during a bacterial response to implicate a possible role in this process. Interestingly, we found that *foxq1a*, but not *foxq1b*, was significantly downregulated by about a factor of 2 in wildtype larvae after LPS or bacteria injection (Fig 5B).

To analyze the immune response of *foxq1* mutants, we employed the brain challenge assay on 4 dpf larval progenies of *foxq1a^{bcz11/+}* and *foxq1b^{bcz18/+}* single and double heterozygous incrosses (Fig 5C). We found that the expression levels of immune activation genes (*il1β*, *irg1*, *mpx, and tnfα*) in *foxq1* mutants at 6 hpi were not significantly different from WT siblings (Fig 5C). However, we cannot exclude the possibility that double *foxq1a* and *foxq1b* mutants may have deficient or aberrant transcriptional response to *E. coli*. Since *foxq1a* transcriptional level was downregulated in wildtype response to *E. coli* (Fig 5B), we also assessed whether this occurred normally in *foxq1* mutants as compared to WT siblings. qPCR data shows that *foxq1b* mutants had similar *foxq1a* expression as WT controls after bacterial exposure, but both heterozygous and homozygous *foxq1a* mutants had a modest but significant increase of ~50% in *foxq1a* RNA level (Fig 5C). The *foxq1a* upregulation was also found in *foxq1a* mutants at steady state, suggesting that the increase during the bacterial response may be due to an already higher baseline level rather than necessarily the bacterial exposure (S3 Fig). The results indicate that *foxq1a* and *foxq1b* may not be required for mediating an appropriate transcriptional response
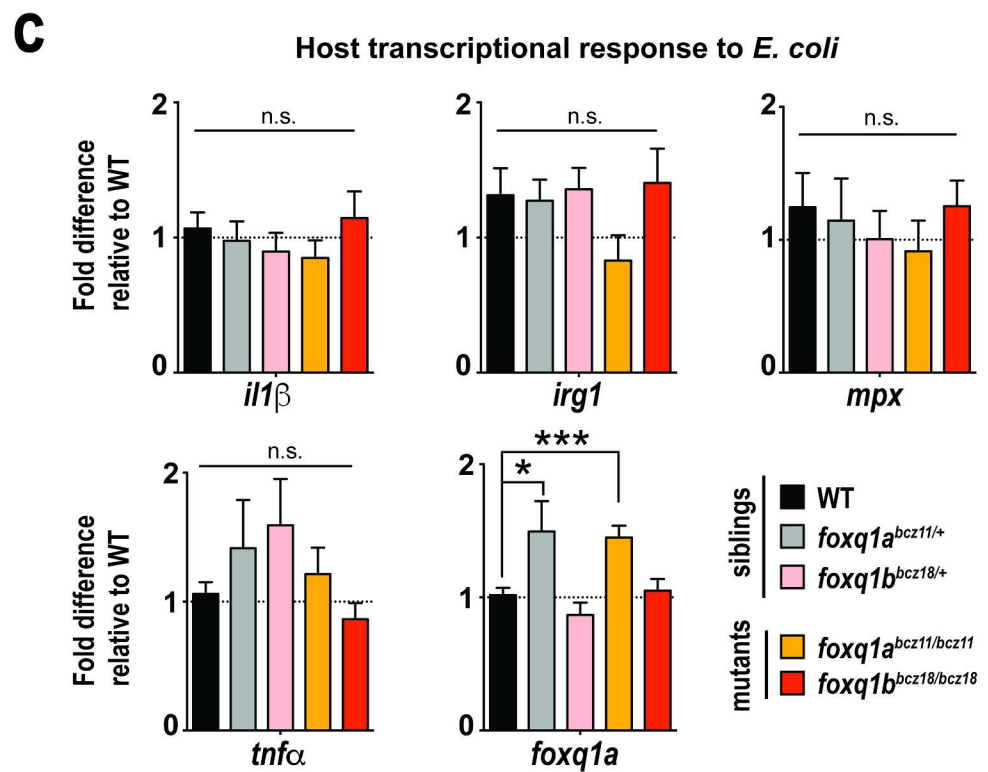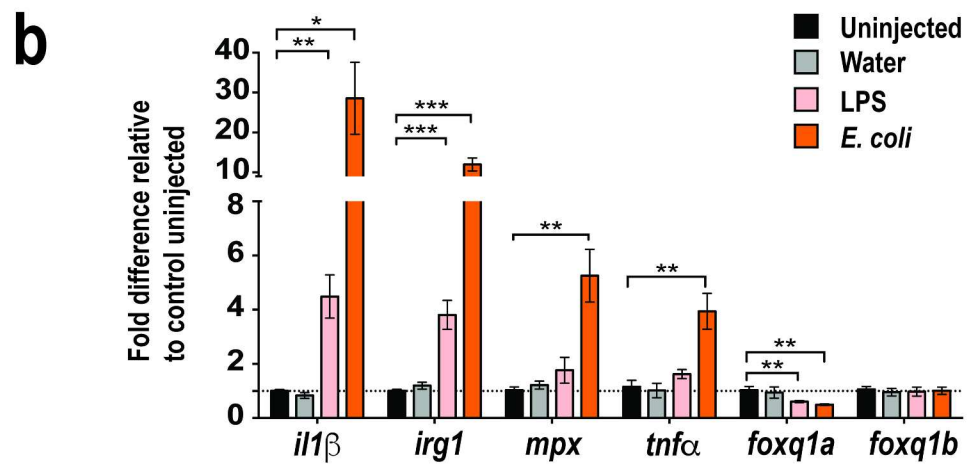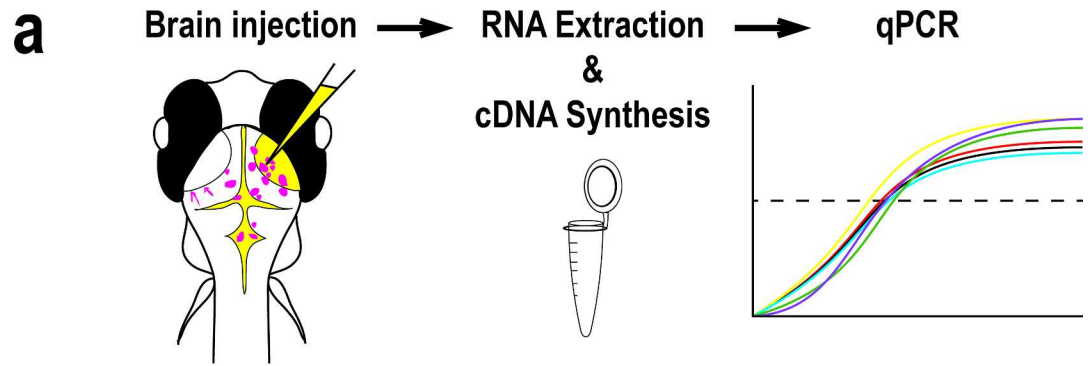
Fig 5. *foxq1a*[bcz11] and *foxq1b*[bcz18] mutants exhibit wildtype transcriptional response to *E. coli* challenge in the larval brain. **a** Graphical representation of the brain challenge assay. *E. coli* was injected into right brain tectum, and at 6 hours post injection (hpi), injected larvae were individually processed for RNA extraction, genotyping, cDNA synthesis, and qPCR analysis. **b** Bar chart shows significant upregulation of immune activation genes *il1β*, *irg1*, *mpx*, and *tnfα* after bacteria challenge at 6 hpi in wildtype larvae compared with uninjected controls. Water injected wildtype larvae exhibit no induction of activation genes, whereas LPS injected wildtype animals have a significant upregulation of *il1β* and *irg1*. After microbial activation by *E. coli* or LPS, a significant downregulation of *foxq1a* was found by about a factor of 2. No significant change was found for *foxq1b* after immune challenge. Data from wildtype injections validate the efficacy of the assay to activate the innate immune system. Dotted line marks no fold difference at 1. At least 6 or more independent biological samples were measured per category. **c** Bar plot shows transcriptional changes of target genes after *E. coli* injection in the brain at 6 hpi for control siblings and *foxq1a* and *foxq1b* mutants. n = 9–14 independent biological samples were measured per genotype. All error bars show standard error of means. Statistical significance in **b** and **c** was determined by multiple unpaired t-tests comparing between uninjected or sibling controls and the experimental groups with correction for multiple comparisons using the Sidak-Bonferroni method and without assuming equal variance. n.s., no statistical significance as defined by p > 0.05. *, p < 0.05; **, p < 0.01; ***, p < 0.001.

https://doi.org/10.1371/journal.pone.0194207.g005

to *E. coli* challenge, but *foxq1a* may affect other aspects of this bacterial response as it is transcriptionally regulated.

Discussion

Our study used zebrafish genetic mutants to investigate the possibility that FOXQ1 may have a role in innate immune cell development and function. Using our newly generated null mutations of the zebrafish homologs of human FOXQ1, *foxq1a* and *foxq1b*, we reveal that these genes are not required for the normal development and distribution of macrophages, neutrophils, and microglia. Furthermore, our data suggests that these two genes are not necessary for a stereotypical transcriptional response to *E. coli* exposure, albeit deficiency in both copies of *foxq1* was not assessed. It is possible, however, that *foxq1a* and *foxq1b* may have important roles in other innate immune functions such as during an infection or injury that were not examined in this study, which include cell migration and recruitment, phagocytosis, and host response to pathogens, viruses, fungi, and environmental toxins. Since *foxq1a* expression was found in macrophages and downregulated during a bacterial response, *foxq1a* may have a role in innate immunity that remains to be fully explored in zebrafish. Furthermore, we show that *foxq1a* is upregulated in the *foxq1a* mutants at steady state and during a bacterial response. This suggests that *foxq1a* may be forming a negative feedback loop in negatively regulating its own transcription.

The *foxq1a*[bcz11] and *foxq1b*[bcz18] mutants will provide useful genetic models to address previously unanswered questions regarding function of zebrafish *foxq1* in craniofacial development, possible gastrointestinal processes, and later adult organogenesis [51,52]. Consistent with the possibility that FOXQ1 has multiple roles in development, FOXQ1/Foxq1 is highly expressed in mouse stomach and kidney, and human gastric mucosa, bladder, salivary glands, trachea, intestines, and liver [2,16,70]. In addition, murine Foxq1 deletion mutants have deficiencies in gastric acid secretion and hair differentiation, and show partial penetrance for embryonic lethality [16,70]. The zebrafish *foxq1* mutants can also be invaluable for uncovering mechanisms mediating the role of FOXQ1 in cancer biology that remains poorly understood.

Materials and methods

Zebrafish lines and embryos

Embryos from wildtype (TL and AB), transgenic lines: *mpeg1:EGFP* [58,71] and *gata1:DsRed* [72], and heterozygous lines: *foxq1a*[bcz11/+], *foxq1b*[bcz18/+], and *foxq1a*[bcz11/+] *foxq1b*[bcz18/+] were raised at 28.5°C, and staged as described [73]. Homozygous mutants were derived from either single heterozygous incrosses or from double heterozygous incrosses. The latter yielded double

foxq1a[bcz11] *foxq1b*[bcz18] mutants at a ratio of ~ 1/16. Embryos were treated with 0.003% 1-phentyl-2-thiourea (PTU) to inhibit pigmentation in sterilized zebrafish system water. This study was carried out in accordance with the animal protocol (16–160) approved by the Institute Animal Care and Use Committee at UNC Chapel Hill.

Neutral red analysis

Microglia were scored in live larvae by neutral red vital dye staining assay as previously described [61,62]. In brief, 3 dpf larvae were stained with neutral red by immersion in system water supplemented with 2.5 μg/ml neutral red and 0.003% PTU at 28.5˚C for 1 hour, followed by 1–2 water changes, and then analyzed 2–3 hours later using a stereomicroscope.

Whole mount RNA *in situ* hybridization

In situ hybridization was performed using standard methods as described in [61,62,74]. Antisense riboprobes were transcribed from: *mfap4* plasmid previously cloned [61], *mpx* (full-length, Open Biosystems clone 6960294) [61], *foxq1a* plasmid (pCES150), which was made from a 877 bp fragment cloned from a wildtype zebrafish embryo cDNA library using primers F476: GCACTCATCATCTGCAACAGGTA and R1353: TGATATCCCGCGGTTGCAGG. Anti-sense *foxq1a* RNA probe was made from pCES150 digested with HindIII and transcribed by T7 RNA polymerase. To make the negative control RNA probe, *foxq1a* sense strand sequence was transcribed by T3 RNA polymerase using a PCR template made from the *foxq1a* plasmid pCES150. *foxq1b* anti-sense RNA probe was made from a PCR-based template encompassing 754 bp of coding sequence using forward primer: GTGTTGCGAGAT CCCTCGCGTC and reverse primer: GTAAACACTGTGCAGTGGCGCGTC, where the reverse primer also included the T7 RNA polymerase recognition site.

RNA extraction, RT-PCR and quantitative PCR (qPCR)

Total RNA was extracted from individual larvae using the RNAqueous-Micro Isolation Kit (Ambion). cDNA was made using oligo dT primer and SuperScript IV reverse transcriptase (Invitrogen). qPCR was performed on the Applied Biosystems QuantStudio Flex 6 Real-Time PCR System using probe-based assays or SYBR Green. The delta–delta ct method was used to determine the relative levels of mRNA expression between experimental samples and controls. *ef1a* was used as the reference gene for determination of relative expression of all target genes. Sequences of the qPCR probes and primer sets used in qPCR and RT-PCR analyses are listed in Table 1.

CRISPR-Cas9 targeted mutagenesis of *foxq1a* and *foxq1b*

The target genes were *foxq1a* (NCBI accession: NM_001243344.1; Gene ID: 100537750) and *foxq1b* (NCBI accession: NM_212907.1; Gene ID: 405843). Co-injection of Cas9 mRNA and guide RNAs (gRNAs) was conducted in wildtype 1-cell stage zebrafish embryos. Cas9 mRNA was transcribed from XbaI linearized pT3TS-nCas9n plasmid (Addgene #46757) [53] using mMessage mMachine T3 Kit (Ambion) according to the manufacturer's instructions. CRISPR targets for gRNA designs were identified using CHOPCHOP (http://chopchop.cbu.uib.no) [54]. The following gene-specific oligonucleotides using T7 promoter were used to make gRNAs as previously described [54]; gene-specific target sequences are underlined: *foxq1a* gRNA-1 5′–TAATACGACT CACTATAGGGTTCGAAGAGTGACAGGGGTTTTAGAGCTAGAAA TAGCAAG–3′, *foxq1a* gRNA-2 5′–TAATACGACTCACTATAGGACTACGACTCCAAGCCT GGTTTTAGAGCTAGAAATAGC AAG–3′, *foxq1a* gRNA-3 5′– TAATACGACTCACTATAGG AGTTGTGCAGCGATGCTGGTTTT AGAGCTAGAAATAGCAAG–3′, *foxq1b* gRNA-1 5′–TAA

Table 1. Probes and primer sequences for qPCR and RT-PCR.

ef1a	probe	CTGGAGACAGCAAGAACGACCCAC	
	F primer	ACATCCGTCGTGGTAATGTG	
	R primer	TGATGACCTGAGCGTTGAAG	
il1b	probe	TCCGTCAAATGTCCCGGTTGGTTTA	
	F primer	ACCGGCAGCTCCATAAAC	
	R primer	GGTGTCTTTCCTGTCCATCTC	
irg1	probe	TTTAACACCGTGCTTCAGTGCAGC	
	F primer	ACTGGGAGTGGGTTTGATTG	
	R primer	GCATACTGAGGTGGAAGAGATG	
mpx	probe	TATAGCATGGTCACGCCCTCTTTGC	
	F primer	TGCCTTCACATCCCACATAG	
	R primer	GGAGCAGACAATCCACAGAA	
tnfa	F primer	GCGCTTTTCTGAATCCTACG	
	R primer	TGCCCAGTCTGTCTCCTTCT	
foxq1a	probe	TAAGGGATCCTTCGAGACCGTGGG	
	F primer	GTGCGCCATAATCTGTCTCTAA	
	R primer	CGGGTTCAGCATCCAGTAAT	
foxq1b	probe	ATGGGATTTCCGCCACAGAGCA	
	F primer	TCCTCACTTTCTGCCAGTTG	
	R primer	ACATTCGACACCTCAGAACTG	
DsRed	F primer	TCCGAGGACGTCATCAAGGAGTTC	sorted cells
	R primer	GGCGGGGTGCTTCACGTACAC	sorted cells
foxq1a	foxq1a_F531	GCAGAAGGAGAAAGCGCATTAG	sorted cells
	foxq1a_R773	AGGATCGAAGCATGACATACGG	sorted cells
foxq1b	foxq1b_F540	CAGCGAGTACACTTTTGCAGAC	sorted cells
	foxq1b_R839	AATCTGCTCTGTGGCGGATAG	sorted cells
GFP	F primer	TATATCATGGCCGACAAGCA	sorted cells
	R primer	CTGGGTGGCTCAGGTAGTGG	sorted cells
hbbe1.1	hbbe1.1_F139	GCTCTGGCAAGGTGTCTCATC	sorted cells
	hbbe1.1_R465	AGCGATGAATTTCTGGAAAGCG	sorted cells
irf8	irf8-218-F	CAGCGACATGGAAGACCAGATTG	sorted cells
	irf8-647-R	GTGGTCACCATGTTGTCCACCATC	sorted cells
mpeg1	mpeg1_F1	ACAACACCACCTTGTTACACTCT	sorted cells
	mpeg1_R1	ACAACTGCTGGATTTGGTCAATG	sorted cells
foxq1a	foxq1a_F476	TGATATCCCGCGGTTGCAGG	2dpf/8dpf/gut
	foxq1a_R1353	GCACTCATCATCTGCAACAGGTA	2dpf/8dpf/gut
foxq1b	foxq1b_F159	ATGGATGTGAACGTGGCTTCA	2dpf/8dpf/gut
	foxq1b_R961	GGGTGAAATCCAGCCTCTTGTA	2dpf/8dpf/gut

TACGACTCACTATAGG<u>CTTCACCGCTGTCCACG</u>GGTTTTAGAGCTAGAAATAGCAAG–3',
foxq1b gRNA-2 5'–TAATACGACTCACTATAGG<u>TTCCTCCTCCGTGGACAG</u>GTTTTAGAGCTA
GAAATAGCAAG–3',*foxq1b* gRNA-3 5'–TAATACGACTCACTATAGG<u>AGCCCAATTCCTCCT
CCG</u>GTTTTAGAGCTAGAAATAGCAAG–3'. In vitro transcription of gRNAs from assembled
oligonucleotides was conducted using the HiScribe T7 Quick High Yield RNA Synthesis Kit
(NEB). Injected clutches of embryos validated to contain CRISPR mediated mutagenesis by a
T7 endonuclease assay were raised as F0 fish. Incross and outcross of F0 adults produced F1
progenies, which were genotyped and sequenced at adult stages to identify F1 founders

carrying mutations of interest. These founders were isolated and outcrossed to raise new mutant lines, which yielded the *foxq1a*^{*bcz11/+*} and *foxq1b*^{*bcz18/+*} heterozygous fish used in this study.

Cell dissociation and fluorescence activated cell sorting (FACS)

Dissociation of pools of 25–50 2.5 dpf transgenic zebrafish embryos either carrying the macrophage reporter (*mpeg1:EGFP*) or the erythrocyte reporter (*gata1:DsRed*) was conducted using a protocol adapted from [75]. Fluorescently tagged cells were sorted from non-fluorescent cells using the BD FACSAria cell sorter equipped with three lasers. Non-fluorescent control embryos were used for setting gates in FACS for GFP and DsRed positive cells. BD FACSDiva V8.0.1 software was used for cell sorting and FACS plots. Total RNA was extracted from the different populations of cells (GFP positive, GFP negative, DsRed positive, DsRed negative) using the RNAqueous-Micro Isolation Kit (Ambion), and made into cDNA for RT-PCR analyses as described above.

Genotyping bcz11 and bcz18 alleles

To genotype *foxq1a*^{*bcz11*}, the following primers were used: *foxq1a F* 5′-CGGTGTTTTTGTGAC TTGATTT-3′ and *foxq1a R* 5′-AAGAGTATGGAGGTTTGGGTCTC-3′ in a PCR assay that yielded differentially sized products to distinguish the mutant allele which has a 95 bp deletion compared with the wildtype allele. The expected sizes for mutant band is 240 bp and wildtype band is 335 bp. To genotype *foxq1b*^{*bcz18*}, a PCR and restriction enzyme combined assay was used. Primers *foxq1b F* 5′-AAGCAACTCATCTGACCTGACA-3′ and *foxq1b R* 5′-GGGTCTA CGCGTATATGGTTTC-3′ were used to yield PCR products of 217 bp, followed by a digest with BsaJI, which only recognizes the wildtype sequence.

Immune challenge

Bacteria were prepared from 3 mL overnight cultures, each derived from a single *Escherichia coli* colony, which were centrifuged and re-suspended in 500 μL of PBS. The 500 μL bacteria mix (~1.6 x 10⁶ cfu/μL) was supplemented with 1 μL of 5 mg/ml AlexaFluor 568 or AlexaFluor 488 conjugated dextran (10 kDa) from Invitrogen. Other reagents used for brain injections were: ultra-pure water supplemented with 0.05 mg/ml fluorescently labeled dextran (10 kDa) for the control water samples, and lipopolysaccharides (LPS) derived from 0111:B4 *E. coli* (L3024 Sigma) at 4.5 mg/ml was supplemented with 0.05 mg/ml fluorescently labeled dextran (10 kDa). For all injections, 1 nL of the reagent mix was injected into the right brain tectum of 4 dpf larvae, and the fluorescent dextran was used to validate the injection site. Larvae that were successfully injected were collected 6 hours post injection (hpi) and immediately processed for total RNA lysis. RNA extraction and subsequent steps for qPCR analyses are described above. All collected larvae derived from heterozygous intercrosses were genotyped after RNA extraction.

Supporting information

S1 Fig. RT-PCR and Sanger sequencing analyses of the mutations *bcz11* and *bcz18* confirm the expression of the expected mutant transcripts and show no alternative splicing. Primers used to amplify the approximate full-length coding region of each gene were: start-F 5′-G CACTCATCATCTGCAACAGGTA and end-R 5′-TGATATCCCGCGGTTGCAGG for *foxq1a* (~900 bp); and start-F 5′-AAGCAACTCATCTGACCTGACA and end-R 5′-GTAAACACTGTG CAGTGGCGCGTC for *foxq1b* (~1150 bp). (a) Inverted DNA gel image of the RT-PCR analysis

of *foxq1a* mRNA shows the expected ~900 bp transcript in WT siblings and a single mutant transcript with a 95 bp deletion in homozygous *bcz11* mutants, indicating no alternative splicing in the mutants. Gel image shows 2 independent samples per genotype. (b) Sanger sequencing analysis of the *foxq1a* transcript from four *bcz11* mutants shows the expected 95 bp deletion that caused a frameshift leading to an early stop codon at the beginning of the gene. (c) RT-PCR analysis of the *foxq1b* transcript in WT and *bcz18* mutants shows the expected product size of ~1150 bp and no apparent splice variants. Gel image shows 2 independent samples per genotype. (d) Sanger sequencing analysis of the *foxq1b* transcript from four *bcz18* mutants confirms the indel mutation that leads to a frameshift and early stop codon. aa, amino acid; sib, sibling; Mut, mutant.
(TIF)

S2 Fig. RNA expression pattern of *foxq1a* and *foxq1b* in zebrafish embryos. a-d *foxq1a* gene expression. **a** Expression in ventral head region is found in 1.5 dpf embryo (arrow). **b** Prominent expression at 2.5 dpf in the craniofacial region (arrows, higher magnification in **c**), on the yolk (arrows, higher magnification in **d**), and along the body abutting the yolk. Yolk expression is not found in all embryos analyzed whereas the craniofacial expression is. **e-f** As a negative control, whole mount in situ hybridization using the sense RNA probe for *foxq1a* does not show any expression at all stages analyzed from 1–3 dpf. **g** *foxq1b* expression is prominent in the craniofacial jaw region. Left, lateral view (arrow). Right, ventral view (arrows).
(TIF)

S3 Fig. *foxq1a* is transcriptionally upregulated in *foxq1a* mutants. A modest upregulation of *foxq1a* RNA expression at ~ 44% on average is found in *foxq1a* mutants at 4 dpf at steady state in the absence of any immune challenge. n = 6 independent biological samples were measured per genotype. All error bars show standard error of means.
(TIF)

Acknowledgments

Author Contributions

Conceptualization: Celia E. Shiau.

Formal analysis: Alison M. Earley, Celia E. Shiau.

Funding acquisition: Celia E. Shiau.

Investigation: Alison M. Earley, Cameron T. Dixon.

Methodology: Celia E. Shiau.

Project administration: Celia E. Shiau.

Validation: Alison M. Earley, Cameron T. Dixon, Celia E. Shiau.

Writing – original draft: Alison M. Earley, Celia E. Shiau.

Writing – review & editing: Alison M. Earley, Cameron T. Dixon, Celia E. Shiau.

References

1. Kaestner KH, Knochel W, Martinez DE. Unified nomenclature for the winged helix/forkhead transcription factors. Genes Dev. 2000; 14: 142–146. PMID: 10702024

2. Bieller A, Pasche B, Frank S, Glaser B, Kunz J, Witt K, et al. Isolation and characterization of the human forkhead gene FOXQ1. http://dx.doi.org/101089/10445490152717596. 2001; 20: 555–561. https://doi.org/10.1089/104454901317094963

3. Katoh M, Katoh M. Human FOX gene family (Review). Int J Oncol. Spandidos Publications; 2004; 25: 1495–1500. https://doi.org/10.3892/ijo.25.5.1495 PMID: 15492844

4. Wotton KR, Mazet F, Shimeld SM. Expression of FoxC, FoxF, FoxL1, and FoxQ1 genes in the dogfish Scyliorhinus canicula defines ancient and derived roles for Fox genes in vertebrate development. Dev Dyn. 2008; 237: 1590–1603. https://doi.org/10.1002/dvdy.21553 PMID: 18498098

5. Jackson BC, Carpenter C, Nebert DW, Vasiliou V. Update of human and mouse forkhead box FOX gene families. Human Genomics 2010 4:5. BioMed Central; 2010; 4: 345. https://doi.org/10.1186/1479-7364-4-5-345 PMID: 20650821

6. Zhang H, Meng F, Liu G, Bin Zhang, Zhu J, Wu F, et al. Forkhead Transcription Factor Foxq1 Promotes Epithelial–Mesenchymal Transition and Breast Cancer Metastasis. Cancer Res. American Association for Cancer Research; 2011; 71: 1292–1301. https://doi.org/10.1158/0008-5472.CAN-10-2825 PMID: 21285253

7. Zhang H, Meng F, Liu G, Zhang B, Zhu J, Wu F. Cross-species expression profiling identifies Forkhead-Box Q1 as a promoter of epithelial-mesenchymal transition and breast cancer metastasis. 2011.

8. Fan D-M, Feng X-S, Qi P-W, Chen Y-W. Forkhead factor FOXQ1 promotes TGF-β1 expression and induces epithelial-mesenchymal transition. Mol Cell Biochem. 2014; 397: 179–186. https://doi.org/10.1007/s11010-014-2185-1 PMID: 25287361

9. Feuerborn A, Srivastava PK, Küffer S. The Forkhead factor FoxQ1 influences epithelial differentiation. Journal of cellular 2011. https://doi.org/10.1002/jcp.22385/full

10. Feuerborn A. The Forkhead factor FoxQ1 influences epithelial plasticity and modulates TGF-beta1 signalling. 2010.

11. Qiao Y, Jiang X, Lee ST, Karuturi RKM, Hooi SC, Yu Q. FOXQ1 Regulates Epithelial-Mesenchymal Transition in Human Cancers. Cancer Res. American Association for Cancer Research; 2011; 71: 3076–3086. https://doi.org/10.1158/0008-5472.CAN-10-2787 PMID: 21346143

12. Hoggatt AM, Kriegel AM, Smith AF, Herring BP. Hepatocyte nuclear factor-3 homologue 1 (HFH-1) represses transcription of smooth muscle-specific genes. J Biol Chem. 2000; 275: 31162–31170. https://doi.org/10.1074/jbc.M005595200 PMID: 10896677

13. Hong HK, Noveroske JK, Headon DJ, Liu T, Sy MS, Justice MJ, et al. The winged helix/forkhead transcription factor Foxq1 regulates differentiation of hair in satin mice. Genesis. 2001; 29: 163–171. https://doi.org/10.1002/gene.1020 PMID: 11309849

14. Potter CS, Peterson RL, Barth JL, Pruett ND. Evidence that the satin hair mutant gene Foxq1 is among multiple and functionally diverse regulatory targets for Hoxc13 during hair follicle differentiation. Journal of Biological . . .. 2006.

15. Verzi MP, Khan AH, Ito S, Shivdasani RA. Transcription Factor Foxq1 Controls Mucin Gene Expression and Granule Content in Mouse Stomach Surface Mucous Cells. Gastroenterology. 2008; 135: 591–600. https://doi.org/10.1053/j.gastro.2008.04.019 PMID: 18558092

16. Goering W, Adham IM, Pasche B, Manner J, Ochs M, Engel W, et al. Impairment of gastric acid secretion and increase of embryonic lethality in Foxq1-deficient mice. Cytogenet Genome Res. 2008; 121: 88–95. https://doi.org/10.1159/000125833 PMID: 18544931

17. Cui Y, Qiao A, Jiao T, Zhang H, Xue Y, Zou Y, et al. The hepatic FOXQ1 transcription factor regulates glucose metabolism in mice. Diabetologia. 2016; 59: 2229–2239. https://doi.org/10.1007/s00125-016-4043-z PMID: 27421728

18. Jonsson H, Peng SL. Forkhead transcription factors in immunology. Cell Mol Life Sci. 2005; 62: 397–409. https://doi.org/10.1007/s00018-004-4365-8 PMID: 15719167

19. Wang P, Lv C, Zhang T, Liu J, Yang J, Guan F, et al. FOXQ1 regulates senescence-associated inflammation via activation of SIRT1 expression. Cell Death Dis. 2017; 8: e2946. https://doi.org/10.1038/cddis.2017.340 PMID: 28726780

20. Kim S-H, Kaschula CH, Priedigkeit N, Lee AV, Singh SV. Forkhead Box Q1 Is a Novel Target of Breast Cancer Stem Cell Inhibition by Diallyl Trisulfide. J Biol Chem. 2016; 291: 13495–13508. https://doi.org/10.1074/jbc.M116.715219 PMID: 27129776

21. Sehrawat A, Kim SH, Vogt A, Singh SV. Suppression of FOXQ1 in benzyl isothiocyanate-mediated inhibition of epithelial–mesenchymal transition in human breast cancer cells. Carcinogenesis. 2012.

22. Abba M, Patil N, Rasheed K, Nelson LD, Mudduluru G. A direct regulation of Twist1 by FOXQ1 promotes colorectal cancer metastasis. 2013.

23. Weng W, Okugawa Y, Toden S, Toiyama Y, Kusunoki M, Goel A. FOXM1 and FOXQ1 Are Promising Prognostic Biomarkers and Novel Targets of Tumor-Suppressive miR-342 in Human Colorectal Cancer. Clin Cancer Res. 2016; 22: 4947–4957. https://doi.org/10.1158/1078-0432.CCR-16-0360 PMID: 27162244

24. Peng X, Luo Z, Kang Q, Deng D, Wang Q, Peng H, et al. FOXQ1 mediates the crosstalk between TGF-β and Wnt signaling pathways in the progression of colorectal cancer. Cancer Biol Ther. 2015; 16: 1099–1109. https://doi.org/10.1080/15384047.2015.1047568 PMID: 25955104

25. Liu JY, Wu XY, Wu GN, Liu F-K, Yao X-Q. FOXQ1 promotes cancer metastasis by PI3K/AKT signaling regulation in colorectal carcinoma. Am J Transl Res. 2017; 9: 2207–2218. PMID: 28559972

26. Bao B, Azmi AS, Aboukameel A, Ahmad A. Pancreatic cancer stem-like cells display aggressive behavior mediated via activation of FoxQ1. Journal of Biological . . . . 2014.

27. Zhan H-X, Xu J-W, Wang L, Wu D, Zhang G-Y, Hu S-Y. FoxQ1 is a Novel Molecular Target for Pancreatic Cancer and is Associated with Poor Prognosis. Curr Mol Med. 2015; 15: 469–477. PMID: 26122655

28. Zhang J, Liu Y, Zhang J, Cui X, Li G, Wang J, et al. FOXQ1 promotes gastric cancer metastasis through upregulation of Snail. Oncol Rep. 2016; 35: 3607–3613. https://doi.org/10.3892/or.2016.4736 PMID: 27109028

29. Xiang X-J, Deng J, Liu Y-W, Wan L-Y, Feng M, Chen J, et al. MiR-1271 Inhibits Cell Proliferation, Invasion and EMT in Gastric Cancer by Targeting FOXQ1. Cell Physiol Biochem. 2015; 36: 1382–1394. https://doi.org/10.1159/000430304 PMID: 26159618

30. Guo J, Yan Y, Yan Y, Guo Q, Zhang M, Zhang J, et al. Tumor-associated macrophages induce the expression of FOXQ1 to promote epithelial-mesenchymal transition and metastasis in gastric cancer cells. Oncol Rep. 2017. https://doi.org/10.3892/or.2017.5877 PMID: 28791370

31. Soleimani F, Hajjari M, Mohammad Soltani B, Behmanesh M. Up-Regulation of FOXC2 and FOXQ1 Is Associated with The Progression of Gastric-Type Adenocarcinoma. Cell J. 2017; 19: 66–71. https://doi.org/10.22074/cellj.2017.4357 PMID: 28580309

32. ZHU Z, Zhu Z, ZHU Z, PANG Z, XING Y, WAN F, et al. Short hairpin RNA targeting FOXQ1 inhibits invasion and metastasis via the reversal of epithelialmesenchymal transition in bladder cancer. Int J Oncol. 2013; 42: 1271–1278. https://doi.org/10.3892/ijo.2013.1807 PMID: 23403865

33. Xia L, Wu K, Fan D. 581 Sox12, a Direct Target of FoxQ1, Promotes Hepatocellular Carcinoma Metastasis Through up-Regulating TWIST1 and FGFBP1. Gastroenterology; 2015.

34. Huang W, Chen Z, Shang X, Tian D, Wang D, Wu K, et al. Sox12, a direct target of FoxQ1, promotes hepatocellular carcinoma metastasis through up-regulating Twist1 and FGFBP1. Hepatology. 2015; 61: 1920–1933. https://doi.org/10.1002/hep.27756 PMID: 25704764

35. Wang W, He S, Ji J, Huang J, Zhang S. The prognostic significance of FOXQ1 oncogene overexpression in human hepatocellular carcinoma. Pathology-Research and. . . . 2013.

36. Zhang J, Yang Y, Yang T, Yuan S, Wang R, Pan Z, et al. Double-negative feedback loop between microRNA-422a and forkhead box (FOX)G1/Q1/E1 regulates hepatocellular carcinoma tumor growth and metastasis. Hepatology. 6 ed. 2015; 61: 561–573. https://doi.org/10.1002/hep.27491 PMID: 25251503

37. Xiao B, Liu H, Gu Z, Ji C. Expression of microRNA-133 inhibits epithelial-mesenchymal transition in lung cancer cells by directly targeting FOXQ1. Arch Bronconeumol. 2016; 52: 505–511. https://doi.org/10.1016/j.arbres.2015.10.016 PMID: 26858166

38. Feng J, Zhang X, Zhu H, Wang X, Ni S, Huang J. FoxQ1 Overexpression Influences Poor Prognosis in Non-Small Cell Lung Cancer, Associates with the Phenomenon of EMT. Kalinichenko VV, editor. PLoS ONE. 2012; 7: e39937. https://doi.org/10.1371/journal.pone.0039937 PMID: 22761930

39. Herlinger AL, Gao M, Wu RC, Wang TL, Rangel L. Abstract A80: NAC1 attenuates BCL6 negative autoregulation and functions as a BCL6 coactivator of FOXQ1 transcription in ovarian cancer (OVCA). 2016.

40. Gao M, Shih I-M, Wang T-L. The role of forkhead box Q1 transcription factor in ovarian epithelial carcinomas. Int J Mol Sci. 2012; 13: 13881–13893. https://doi.org/10.3390/ijms131113881 PMID: 23203039

41. Sun H-T, Cheng S-X, Tu Y, Li X-H, Zhang S. FoxQ1 Promotes Glioma Cells Proliferation and Migration by Regulating NRXN3 Expression. Jiang T, editor. PLoS ONE. 2013; 8: e55693. https://doi.org/10.1371/journal.pone.0055693 PMID: 23383267

42. Brown JM, Recht L, Strober S. The Promise of Targeting Macrophages in Cancer Therapy. Clin Cancer Res. 2017; 23: 3241–3250. https://doi.org/10.1158/1078-0432.CCR-16-3122 PMID: 28341752

43. Xia L, Chen Z, Liu J, Shang X, Nie Y. Foxq1-ccl2 signaling-induced macrophage recruitment promotes hepatocellular carcinoma metastasis. Journal of . . .; 2013.

44. Ostuni R, Kratochvill F, Murray PJ, Natoli G. Macrophages and cancer: from mechanisms to therapeutic implications. Trends Immunol. 2015; 36: 229–239. https://doi.org/10.1016/j.it.2015.02.004 PMID: 25770924

45. Petty AJ, Yang Y. Tumor-associated macrophages: implications in cancer immunotherapy. Immunotherapy. 2017; 9: 289–302. https://doi.org/10.2217/imt-2016-0135 PMID: 28231720

46. Lewis CE, Harney AS, Pollard JW. The Multifaceted Role of Perivascular Macrophages in Tumors. Cancer Cell. 2016; 30: 365. https://doi.org/10.1016/j.ccell.2016.07.009 PMID: 27505682

47. Mantovani A, Marchesi F, Malesci A, Laghi L, Allavena P. Tumour-associated macrophages as treatment targets in oncology. Nat Rev Clin Oncol. 2017; 14: 399–416. https://doi.org/10.1038/nrclinonc.2016.217 PMID: 28117416

48. Ruffell B, Coussens LM. Macrophages and therapeutic resistance in cancer. Cancer Cell. 2015; 27: 462–472. https://doi.org/10.1016/j.ccell.2015.02.015 PMID: 25858805

49. Kaneda H, Arao T, Tanaka K, Tamura D, Aomatsu K. Overexpression of FOXQ1 is important factor in tumorigenicity and tumor growth. 2010.

50. Li Y, Zhang Y, Yao Z, Li S, Yin Z, Xu M. Forkhead box Q1: A key player in the pathogenesis of tumors (Review). Int J Oncol. 2016; 49: 51–58. https://doi.org/10.3892/ijo.2016.3517 PMID: 27176124

51. Planchart A, Mattingly CJ. 2,3,7,8-Tetrachlorodibenzo-p-dioxin upregulates FoxQ1b in zebrafish jaw primordium. Chem Res Toxicol. 2010; 23: 480–487. https://doi.org/10.1021/tx9003165 PMID: 20055451

52. Topczewska JM, Shoela RA, Tomaszewski JP, Mirmira RB, Gosain AK. The Morphogenesis of Cranial Sutures in Zebrafish. PLoS ONE. 2016; 11: e0165775. https://doi.org/10.1371/journal.pone.0165775 PMID: 27829009

53. Jao L-E, Wente SR, Chen W. Efficient multiplex biallelic zebrafish genome editing using a CRISPR nuclease system. Proc Natl Acad Sci USA. 2013; 110: 13904–13909. https://doi.org/10.1073/pnas.1308335110 PMID: 23918387

54. Gagnon JA, Valen E, Thyme SB, Huang P, Ahkmetova L, Pauli A, et al. Efficient Mutagenesis by Cas9 Protein-Mediated Oligonucleotide Insertion and Large-Scale Assessment of Single-Guide RNAs. Riley B, editor. PLoS ONE. 2014; 9: e98186. https://doi.org/10.1371/journal.pone.0098186 PMID: 24873830

55. Willet SG, Mills JC. Stomach Organ and Cell Lineage Differentiation: from Embryogenesis to Adult Homeostasis. Cell Mol Gastroenterol Hepatol. 2016; 2: 546–559. https://doi.org/10.1016/j.jcmgh.2016.05.006 PMID: 27642625

56. Kim TH, Shivdasani RA. Stomach development, stem cells and disease. Development. 2016; 143: 554–565. https://doi.org/10.1242/dev.124891 PMID: 26884394

57. Walton EM, Cronan MR, Beerman RW, Tobin DM. The macrophage-specific promoter mfap4 allows live, long-term analysis of macrophage behavior during mycobacterial infection in zebrafish. Gong Z, editor. PLoS ONE. 2015; 10: e0138949. https://doi.org/10.1371/journal.pone.0138949 PMID: 26445458

58. Zakrzewska A, Cui C, Stockhammer OW, Benard EL, Spaink HP, Meijer AH. Macrophage-specific gene functions in Spi1-directed innate immunity. Blood. 2010; 116: e1–11. https://doi.org/10.1182/blood-2010-01-262873 PMID: 20424185

59. Lieschke GJ, Oates AC, Crowhurst MO, Ward AC, Layton JE. Morphologic and functional characterization of granulocytes and macrophages in embryonic and adult zebrafish. Blood. 2001; 98: 3087–3096. https://doi.org/10.1182/blood.V98.10.3087 PMID: 11698295

60. Mathias JR, Dodd ME, Walters KB, Yoo SK, Ranheim EA, Huttenlocher A. Characterization of zebrafish larval inflammatory macrophages. Developmental & Comparative Immunology. 2009; 33: 1212–1217. https://doi.org/10.1016/j.dci.2009.07.003 PMID: 19619578

61. Shiau CE, Monk KR, Joo W, Talbot WS. An anti-inflammatory NOD-like receptor is required for microglia development. Cell Rep. 2013; 5: 1342–1352. https://doi.org/10.1016/j.celrep.2013.11.004 PMID: 24316075

62. Shiau CE, Kaufman Z, Meireles AM, Talbot WS. Differential Requirement for irf8 in Formation of Embryonic and Adult Macrophages in Zebrafish. Wen Z, editor. PLoS ONE. 2015; 10: e0117513. https://doi.org/10.1371/journal.pone.0117513 PMID: 25615614

63. Herbomel P, Thisse B, Thisse C. Zebrafish early macrophages colonize cephalic mesenchyme and developing brain, retina, and epidermis through a M-CSF receptor-dependent invasive process. Dev Biol. 2001; 238: 274–288. https://doi.org/10.1006/dbio.2001.0393 PMID: 11784010

64. Meireles AM, Shiau CE, Guenther CA, Sidik H, Kingsley DM, Talbot WS. The phosphate exporter xpr1b is required for differentiation of tissue-resident macrophages. Cell Rep. 2014; 8: 1659–1667. https://doi.org/10.1016/j.celrep.2014.08.018 PMID: 25220463

65. Shen K, Sidik H, Talbot WS. The Rag-Ragulator Complex Regulates Lysosome Function and Phagocytic Flux in Microglia. Cell Rep. Elsevier; 2016; 14: 547–559. https://doi.org/10.1016/j.celrep.2015.12.055 PMID: 26774477

66. Ogryzko NV, Hoggett EE, Solaymani-Kohal S, Tazzyman S, Chico TJA, Renshaw SA, et al. Zebrafish tissue injury causes upregulation of interleukin-1 and caspase-dependent amplification of the inflammatory response. DMM Disease Models and Mechanisms. 2014; 7: 259–264. https://doi.org/10.1242/dmm.013029 PMID: 24203886

67. Hall CJ, Boyle RH, Astin JW, Flores MV, Oehlers SH, Sanderson LE, et al. Immunoresponsive gene 1 augments bactericidal activity of macrophage-lineage cells by regulating β-oxidation-dependent mitochondrial ros production. Cell Metab. 2013; 18: 265–278. https://doi.org/10.1016/j.cmet.2013.06.018 PMID: 23931757

68. Yan B, Han P, Pan L, Lu W, Xiong J, Zhang M, et al. IL-1β and reactive oxygen species differentially regulate neutrophil directional migration and basal random motility in a zebrafish injury-induced inflammation model. Journal of Immunology. 2014; 192: 5998–6008. https://doi.org/10.4049/jimmunol.1301645 PMID: 24835391

69. Zelova H, Hosek J. TNF-alpha signalling and inflammation: interactions between old acquaintances. Inflamm Res. 2013; 62: 641–651. https://doi.org/10.1007/s00011-013-0633-0 PMID: 23685857

70. Frank S, Zoll B. Mouse NHF-3/fork head homolog-1-like gene: Structure, chromosomal location, and expression in adult and embryonic kidney. DNA and Cell Biology. 1998; 17: 679–688. https://doi.org/10.1089/dna.1998.17.679 PMID: 9726250

71. Ellett F, Pase L, Hayman JW, Andrianopoulos A, Lieschke GJ. mpeg1 promoter transgenes direct macrophage-lineage expression in zebrafish. Blood. 2011; 117: e49–56. https://doi.org/10.1182/blood-2010-10-314120 PMID: 21084707

72. Traver D, Paw BH, Poss KD, Penberthy WT, Lin S, Zon LI. Transplantation and in vivo imaging of multi-lineage engraftment in zebrafish bloodless mutants. Nat Immunol. 2003; 4: 1238–1246. https://doi.org/10.1038/ni1007 PMID: 14608381

73. Kimmel CB, Ballard WW, Kimmel SR, Ullmann B, Schilling TF. Stages of embryonic development of the zebrafish. Dev Dyn. 1995; 203: 253–310. https://doi.org/10.1002/aja.1002030302 PMID: 8589427

74. Pogoda H-M, Sternheim N, Lyons DA, Diamond B, Hawkins TA, Woods IG, et al. A genetic screen identifies genes essential for development of myelinated axons in zebrafish. Dev Biol. 2006; 298: 118–131. https://doi.org/10.1016/j.ydbio.2006.06.021 PMID: 16875686

75. Manoli M, Driever W. Fluorescence-activated cell sorting (FACS) of fluorescently tagged cells from zebrafish larvae for RNA isolation. Cold Spring Harb Protoc. 2012; 2012: pdb.prot069633. https://doi.org/10.1101/pdb.prot069633 PMID: 22854565